Dispersive tristability in microring resonators

Yannick Dumeige* and Patrice Féron
Laboratoire d'Optronique (CNRS-UMR 6082 "FOTON") ENSSAT, Université de Rennes 1, 6 rue de Kerampont, BP 80518, 22300 Lannion, France

(Received 20 June 2005; published 16 December 2005)

Combining a transfer matrix analysis and slowly varying envelope approximation, we propose a simple method to describe steady states associated with dispersive multistability in coupled microring resonators. This approach allows us to consider nonlinear interactions between independent forward and backward propagative fields. We applied this simple formalism first to decrease the tristability intensity threshold in linearly coupled resonators and second to optically control the tristable behavior in a single microring resonator.

DOI: 10.1103/PhysRevE.72.066609 PACS number(s): 42.79.−e, 42.65.Wi

I. INTRODUCTION

Nonlinear optical devices are key elements for implementation of ultrafast all-optical signal processing. Microcavities (spheres, disks, rings, and tori) and their associated whispering gallery modes (WGM's) have been well studied in the past few years and are attractive elements for integration of low-threshold nonlinear devices [1]. Recently, Ibrahim *et al.* [2] have demonstrated all-optical switching in microring resonator using the third-order nonlinearity associated with two photon absorption of III-V semiconductor compounds. In this context, dispersive bistability or tristability in microrings can be used to obtain elementary functions such as logical gate, optical switch, or optical memory [3]. Especially tristable devices could be used as building blocks for implementation of ternary optical logic. Stationary behavior of nonresonant multistable optical resonators has been already well studied [4,5]. It is well established that in a single resonator dispersive tristability stems from two resonances separated by one free spectral range (FSR). Consequently the amount of nonlinear phase shift necessary to reach optical tristability is strongly dependent on the FSR. Due to their low dimensions, the FSR of microcavities is very large and the power required to reach tristability can be very high in this kind of resonators. The aim of this paper is first to propose a very simple way to describe nonlinear interactions between two independent forward and backward fields in coupled microrings and second to study conditions to obtain optical tristability in order to reduce its intensity threshold.

Stability in one ring with instantaneous Kerr effect and two linked counterpropagative fields (Sagnac effect) has been studied extensively [6,7], like multistability in a multilayered medium or coupled resonators [8,9]. We focus here on a simple method describing third-order instantaneous nonlinear effects in coupled microring resonators. We combine the 4×4 matrix analysis developed by Poon *et al.* [10] with a nonlinear slowly varying envelope approximation (SVEA). This 4×4 description coming from the particular geometry of ring resonators allows us to consider forward and backward independent nonlinearly coupled fields. In Sec. II, we describe the method used to calculate nonlinear propagation in microrings. In the first part of Sec. III, we start by giving conditions for tristability in a single microring. We then study the different regimes of tristability of two coupled microrings and compare their tristability intensity threshold with the single microring configuration. Section IV is devoted to optically control the tristable regime of a microring benefitting from the "four-port" configuration. Taking into account potential applications of these devices in ultrafast all-optical signal processing, we deliberately chose for our examples structures with moderate quality factors ($Q\sim6.5\times10^3$). Indeed, high Q factors lead to nonnegligible transient regimes with characteristic durations higher than the cavity lifetime [11,12]. Moreover, in this paper we studied steady states associated with dispersive multistability in polymer microrings and practical coupled-microring devices that are being manufactured already have Q factors of approximately 10^4 for polymers.

II. MODEL

We consider a finite chain of N coupled nonlinear microring resonators side coupled with two straight waveguides (see Fig. 1). We assume that waveguides and resonators are single-mode, and therefore the electric field can be represented by its modal envelope everywhere in the structure. We have chosen a notation slightly different from that of Poon *et al.* [10] as we separate directly both contributions for forward and backward propagating waves. If the input field is a_0' (or c_0'), the output field is always b_{N+1} (respectively, d_{N+1}) for a number N (even or odd) of rings. Reciprocally an input

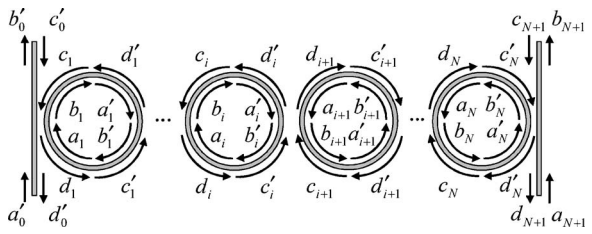

FIG. 1. N microring resonators waveguide side coupled with instantaneous Kerr nonlinearity. For each resonator, forward and backward propagating field envelopes are represented.

*Electronic address: yannick.dumeige@enssat.fr

field a_{N+1} is associated with an output field b_0' (respectively, c_{N+1} to d_0').

A. Coupling between adjacent resonators

For a given microring the electric field is characterized by eight field values. Then, it is possible to define a vector x_i containing theses values in the left part of the resonator and a vector x_i' for the right part. These vectors for a one-frequency component are given by

$$x_i = \begin{bmatrix} a_i \\ b_i \\ c_i \\ d_i \end{bmatrix}, \quad x_i' = \begin{bmatrix} a_i' \\ b_i' \\ c_i' \\ d_i' \end{bmatrix}. \tag{1}$$

The coupling between two adjacent resonators is given by the two following matrix relations [13]:

$$\begin{bmatrix} b_i' \\ b_{i+1} \end{bmatrix} = \mathcal{C}_{i+1} \begin{bmatrix} a_i' \\ a_{i+1} \end{bmatrix}, \quad \begin{bmatrix} d_i' \\ d_{i+1} \end{bmatrix} = \mathcal{C}_{i+1} \begin{bmatrix} c_i' \\ c_{i+1} \end{bmatrix}. \tag{2}$$

Taking into account an asymmetric coupling with losses $\mathcal{C}_{i+1}$ can be written as

$$\mathcal{C}_{i+1} = \begin{bmatrix} t_i' & \kappa_i \\ -\kappa_i'^{*} & t_i^{*} \end{bmatrix}, \quad i \in \{0, \ldots, N\}. \tag{3}$$

Thus we can link x_i' to x_{i+1} using a 4×4 invertible matrix $\mathcal{P}_{i+1}$:

$$x_i' = \mathcal{P}_{i+1} x_{i+1}, \quad \mathcal{P}_{i+1} = \begin{bmatrix} P_{i+1} & 0 \\ 0 & P_{i+1} \end{bmatrix}, \tag{4}$$

with

$$P_{i+1} = \frac{1}{\kappa_i'^{*}} \begin{bmatrix} t_i^{*} & -1 \\ \kappa_i \kappa_i^{*} + t_i^{*} t_i' & -t_i' \end{bmatrix}. \tag{5}$$

As demonstrated by linear and nonlinear finite-difference time domain simulations in previous papers [12,14], the coupling by the optical tunnel effect between waveguides and microrings is not resonant and almost independent on nonlinear phase shift. In the following subsection devoted to nonlinear propagation we assume a linear and local coupling between waveguides and microrings.

B. Nonlinear propagation

We call s the curvilinear abscise along one ring ($s \in [0, 2L_i[$, where L_i is the half perimeter of the ith microring). The total field is the sum of two forward- and backward-propagating fields $F_i(s)$ and $B_i(s)$ (see Fig. 2). The ith nonlinear microring is constituted by an instantaneous, dispersive, local, Kerr material with nonlinear refractive index $N_{2,i}$. By introducing β_i, the propagation constant, and its real part $\mathrm{Re}(\beta_i)$, it is possible to obtain in the SVEA and related approximations (i.e., omission of the nonlinearities in the boundary conditions, of third-order harmonics generation, of the second derivatives and products of first derivatives appearing in the nonlinear wave equation) the differential equations verified by F_i and B_i [6]:

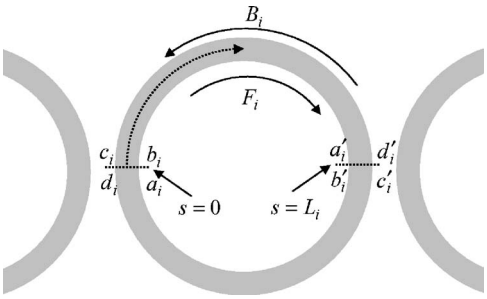

FIG. 2. Propagation along the ith microring. L_i is its half perimeter and s the curvilinear abscise. F_i is the forward-propagating field and B_i the backward one.

$$\frac{dF_i}{ds} = -j\frac{\mathrm{Re}(\beta_i)N_{2,i}\epsilon_0 c}{2}(|F_i|^2 + 2|B_i|^2)F_i - j\beta_i F_i,$$

$$\frac{dB_i}{ds} = j\frac{\mathrm{Re}(\beta_i)N_{2,i}\epsilon_0 c}{2}(|B_i|^2 + 2|F_i|^2)B_i + j\beta_i B_i. \tag{6}$$

β_i is linked to the refractive index n_i, the intensity propagation losses α_i, and the working wavelength λ by

$$\beta_i = 2\pi n_i/\lambda + j\alpha_i/2. \tag{7}$$

The nonlinear propagation along the resonators couples forward and backward propagating fields and the interferences of those fields cause grating based effects. Integrating these two equations along the ith resonator and using the boundary conditions $F_i(0)=b_i$, $B_i(0)=c_i$, $F_i(L_i^-)=a_i'$, $B_i(L_i^-)=d_i'$, $F_i(L_i^+)=b_i'$, $B_i(L_i^+)=c_i'$, $F_i(2L_i^-)=a_i$, and $B_i(2L_i^-)=d_i$ we find

$$a_i = b_i' \exp(-j\beta_i L_i)\exp[-j\gamma_i(2|c_i'|^2/A_i + |b_i'|^2)],$$

$$b_i = a_i' \exp(j\beta_i L_i)\exp[j\gamma_i(|a_i'|^2/A_i + 2|d_i'|^2)],$$

$$c_i = d_i' \exp(-j\beta_i L_i)\exp[-j\gamma_i(2|a_i'|^2/A_i + |d_i'|^2)],$$

$$d_i = c_i' \exp(j\beta_i L_i)\exp[j\gamma_i(|c_i'|^2/A_i + 2|b_i'|^2)]. \tag{8}$$

$A_i=\exp(\alpha_i L_i)$ and γ_i characterize the nonlinear effective properties of the resonator:

$$\gamma_i = \frac{\pi N_{2,i}\epsilon_0 c n_i}{\lambda}\frac{A_i - 1}{\alpha_i}. \tag{9}$$

Note that it is possible to obtain x_i as a function of x_i' because nonlinear effects do not affect the amplitude of the field envelope and therefore $|a_i'|^2=A_i|b_i|^2$ and $|c_i'|^2=A_i|d_i|^2$. Using Eqs. (4) and (8) we link x_{i+1} and x_i. After $N+1$ iterations we can calculate the value of x_0' knowing the value of x_{N+1} and taking into account the nonlinear coupling between forward and backward propagating fields. If we consider only one input a_0', x_{N+1} has only one nonzero component b_{N+1}. Consequently, we can apply the so-called "dummy-variable technique" [9] which allows us to solve the problem analytically. We obtain the field values x_{N+1} and x_0' as a function of

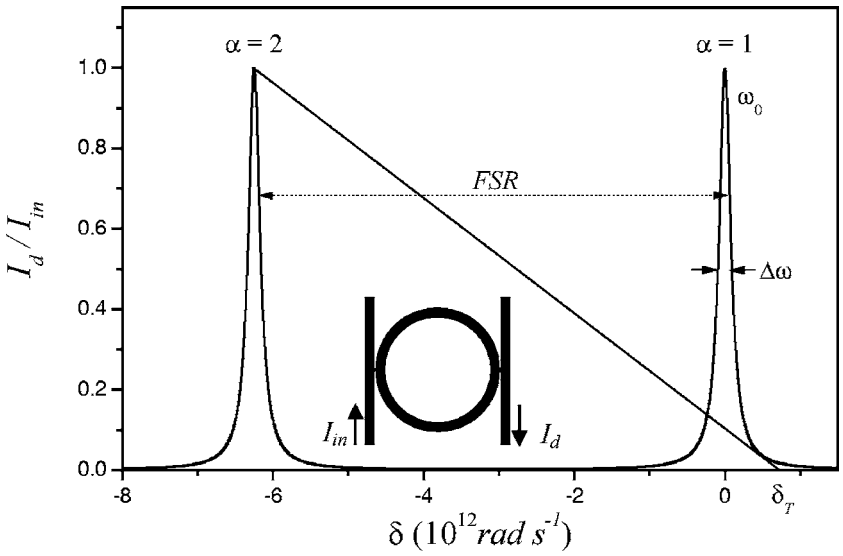

FIG. 3. Single microring (radius $R=30\ \mu$m with $\kappa_0=\kappa_1=0.3j$) transmission as a function of detuning δ. The straight line corresponds to graphical determination of δ_T. This line has exactly three intersections with the linear transmission spectrum and gives the minimal value of δ to obtain tristability.

the single parameter b_{N+1}. This is why we have chosen to calculate x_0' as a function of x_{N+1}.

III. REDUCTION OF THE TRISTABILITY THRESHOLD

We first apply this calculation scheme to the reduction of optical tristabilitythreshold. As in the previous paper [12], the resonators will be made with the same third-order nonlinear polymer material; consequently, all the refractive indices are taken equal to 1.6. In the following examples we will consider that the coupling is symmetric and lossless. Consequently we have $t_i=t_i'$ (real number in the following), $\kappa_i=\kappa_i'$, and $|t_i|^2+|\kappa_i|^2=1$. Furthermore, we consider a nonlinear index N_2 with a negative value and $\alpha_i=0$. Our method is based on the SVEA and the related approximations, in all calculations, except for the upper limit of the second bistable cycle in Sec. III A, and for extrema values of coupling coefficients in Sec. III B, the input intensities and the resonator lengths allow the two conditions discussed by Danckaert *et al.* [9] (i.e., $|\gamma_i||a_i|^2$ and $|\gamma_i||d_i|^2 \ll \beta_i L_i$ and $L_i > \lambda/n_i$) to be fulfilled.

A. Tristability in single microring

We first consider the simplest case of a single resonator with one input field a_0' in a symmetrical dual-coupling configuration. This configuration can lead to bistability [5,12] and multistability for high input power like a Fabry-Perot interferometer filled with a Kerr medium [4]. We define $I_{in}=\frac{1}{2}\epsilon_0 c n_0 |a_0'|^2$ as the input intensity and $I_d=\frac{1}{2}\epsilon_0 c n_2 |b_2|^2$ as the output intensity on the drop port. Figure 3 represents the transmission I_d/I_{in} of the structure in the linear regime. ω_0 is a resonance circular frequency, and $\delta=\omega-\omega_0$ is the detuning between the working angular frequency $\omega=2\pi c/\lambda$ and ω_0. We also define the free spectral range $F_{SR}=\pi c/(n_1 L_1)$, the full width at half maximum $\Delta\omega$ of the linear resonances, and the finesse as $\mathcal{F}=F_{SR}/\Delta\omega$ of the microring. For a detuning $\delta \geqslant \delta_B$ with

$$\delta_B = \frac{F_{SR}\sqrt{3}}{2\mathcal{F}}, \tag{10}$$

one can observe hysteretic cycles associated with cavity resonances spectrally separated by a free spectral range [5].

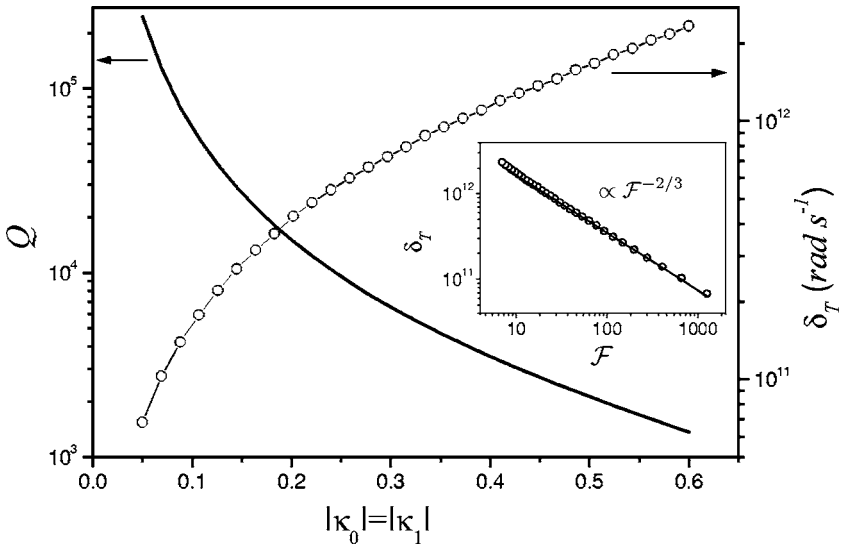

FIG. 4. Q factor (straight line) and δ_T (open circles) as functions of coupling coefficients $\kappa_0=\kappa_1$ in the case of a single resonator ($R=30\ \mu$m) and a forward-propagating field. The inset shows the direct correspondence between $\mathcal{F}$ and δ_T.

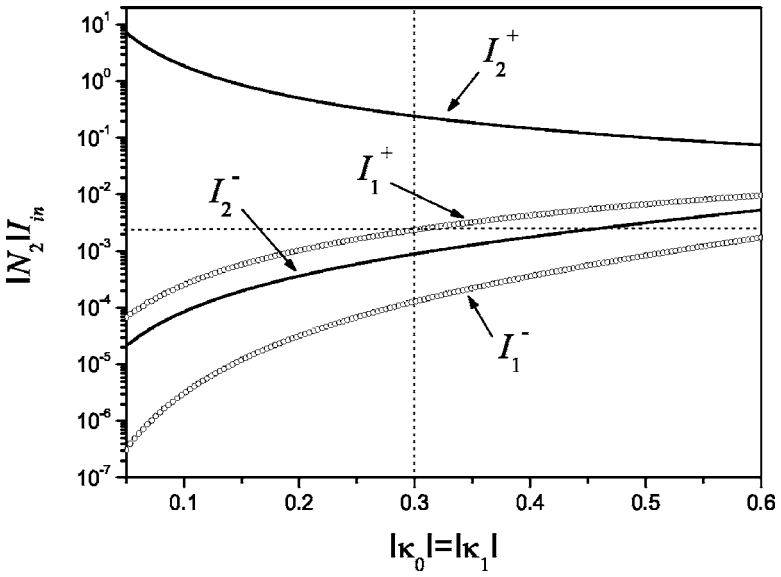

FIG. 5. Switch intensities as a function of the coupling coefficient $|\kappa_0|$ for $\delta > \delta_T$. The vertical and horizontal dotted lines give I_1^+ in the case $\kappa_0=\kappa_1=0.3j$.

Figure 3 shows a typical feature of two cavity resonances with a moderate finesse ($\mathcal{F}\approx 33$). For each resonance, the associated hysteretic cycle (bistable) is limited by incident intensities I_α^+ and I_α^- (switch intensities for resonance or cycle α). They correspond respectively to turn-on and turn-off fields and give us the extension of the instable branches defined by $dI_d/dI_{in}<0$ [7]. If we consider the standard graphical determination method [4] developed to study nonlinear Fabry-Perot (see Fig. 3) and assume the high-finesse approximation, we easily determine the minimal value δ_T of the detuning which corresponds to the condition $I_1^+=I_2^-$:

$$\delta_T = \frac{F_{SR}}{2\sqrt[3]{2\mathcal{F}^2}}\left(3+\frac{1}{2\sqrt[3]{2\mathcal{F}^2}}\right). \tag{11}$$

$\delta > \delta_T$ leads to switch intensities such as $I_2^- < I_1^+$, and one can observe the overlapping of two bistable cycles. This overlapping produces a tristable region. To check relation (11), using the model described in Sec. II and varying coupling coefficients $\kappa_0=\kappa_1$, we numerically evaluate the minimal detuning δ_T (Fig. 4) as well as the quality factor $Q=\omega_0/\Delta\omega$ associated with the device, evaluated using

$$Q = \frac{\pi\omega_0}{F_{SR}}\frac{\sqrt{1-|\kappa_0|^2}}{|\kappa_0|^2}. \tag{12}$$

Note that we fixed the size of the microring, $L_1=\pi R$ ($R=30$ μm), and the resonant wavelength to $\lambda_0\approx 1540$ nm. We represent in the inset of Fig. 4 the minimal detuning δ_T as a function of the finesse. Open circles are calculated numerically and the straight line is deduced from Eq. (11). The superposition of the two curves validates the analytical approach.

Figure 5 represents the switch intensities $I_\alpha^\pm$ with $\alpha \in \{1,2\}$ as a function of the coupling coefficient for a detuning $\delta=1.45\delta_T$. With this detuning choice we always observe tristability because $I_2^- < I_1^+$.

As an example, we consider the case of one resonator with $\kappa_0=\kappa_1=0.3j$. Taking into account the value of L_1 this leads to quality factor $Q=6.5\times 10^3$. Figure 6 shows the transmission I_d/I_{in} as a function of the normalized input intensity $|N_2|I_{in}$ for this single resonator and $\delta=1.45\delta_T$. The area between I_2^- and I_1^+ shows three stable branches (verifying $dI_d/dI_{in}>0$; see Ref. [7]) and can lead to tristability. In this example, tristability is reached for normalized input intensity $|N_2|I_{in}$ greater than 0.2 which corresponds to internal normalized intensity $|N_2|I_{cav}\sim 2.2$. This intensity not only invalidates the SVEA, but material breakdown would also occur with such large refractive index changes. Nevertheless, the results are still qualitatively valid. Note first that the value of I_1^+ is always compatible with the SVEA and so approximations used to establish Eq. (11) are valid. Second, increasing the Q factor (i.e., decreasing $|\kappa_0|$) leads to an increase in the turn-on intensity I_2^+ which corresponds to tristability threshold (see Fig. 5).

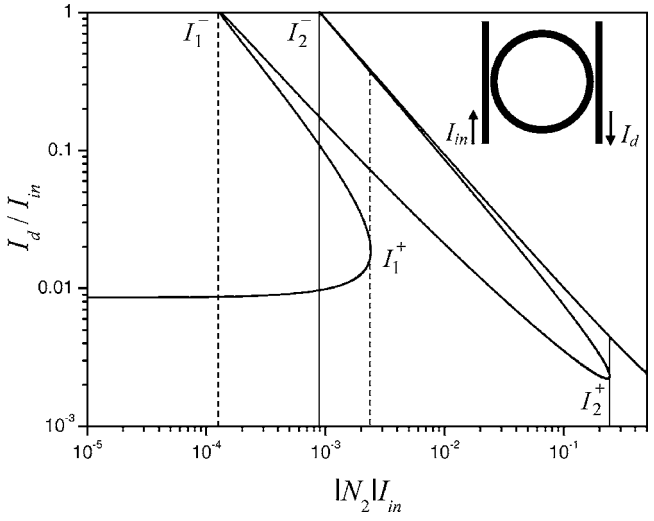

FIG. 6. Transmission as a function of normalized input intensity in the case of a single resonator (mean radius $R=30$ μm with $\kappa_0=\kappa_1=0.3j$) and a forward-propagating field. Dashed and solid vertical lines are the limits of the two bistable cycles.

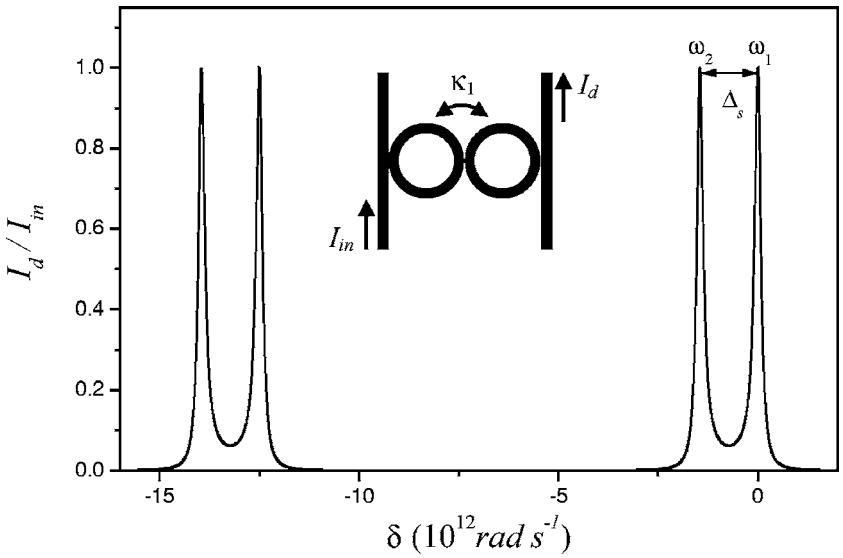

FIG. 7. Linear transmission in the case of two resonators (mean radii $R/2=15$ μm with $\kappa_0=\kappa_2=0.3j$) and a forward-propagating field. $\kappa_1=0.36j$ is the coupling coefficient between the two microrings.

B. Tristability in two coupled microrings

The coupling between two identical microrings in a dual symmetrical coupling configuration with input and output straight waveguides is now considered. In this case $I_{in}=\frac{1}{2}\epsilon_0 c n_0 |a_0'|^2$ and $I_d=\frac{1}{2}\epsilon_0 c n_3 |b_3|^2$. The coupling between two resonators can induce a resonant frequency splitting [15] $\Delta_s < F_{SR}$. This feature is expected to reduce the tristability associated with these multipeaks. The value of Δ_s is strongly dependent on the value of the coupling coefficient between the two rings κ_1. Consequently the tristable behavior of the structure will also depend on this parameter. In order to directly compare this configuration with the former in terms of the Q factor and nonlinear interaction length we have chosen $\kappa_0=\kappa_2=0.3j$ and $L_1=L_2=\pi R/2$. Figure 7 shows the linear response for a moderate coupling coefficient between the two rings ($\kappa_1=0.36j$). To study the tristability, the same absolute detuning $\delta=\omega-\omega_1=1.45\delta_T$ where δ_T is defined for a single ring with $L_1=\pi R$ as in the first example is considered here. For a weak coupling $|\kappa_1| \leqslant 0.1$ there is no or a too small splitting (maximal flatness response occurs for $\kappa_1 \approx 0.05j$), and in the best case, tristability due to overlapping of bistable cycles associated with resonances separated by a quasi-FSR ($\sim$ twice than in the first case) can be reached. The domain of interest corresponds to higher $|\kappa_1|$ values. Figure 8 presents a numerical evaluation of the switch intensities as a function of $|\kappa_1|$. Considering the switch intensities $I_\alpha^\pm$ ($\alpha \in \{1,2\}$) we can distinguish three different regimes. With $0.1 < |\kappa_1| \leqslant 0.3$ (regime I) the bistable cycle overlapping is favored and the tristability threshold (I_2^+) decreases. In regime II ($0.3 < |\kappa_1| \leqslant 0.41$) we obtain $I_2^+ \leqslant I_1^+$ and I_2^+ decreases with $|\kappa_1|$. This leads to a strongly modified hysteretic cycle (one bistable cycle included in another), and tristability is reachable as soon as bistability occurs. For the extremum value $|\kappa_1|=0.41$, the linear transmission presents a large splitting and low values between the split resonances. Consequently the system can be assumed as a single resonator with a double-resonance periodicity. The bistable cycle associated with resonators coupling (regime II) disappears. In regime III ($|\kappa_1| > 0.41$) we obtain an overlapping regime due to a too large splitting and a higher-order cycle; I_2^+ and I_2^- are extensions of I_3^+ and I_3^- in regime II. Values obtained for

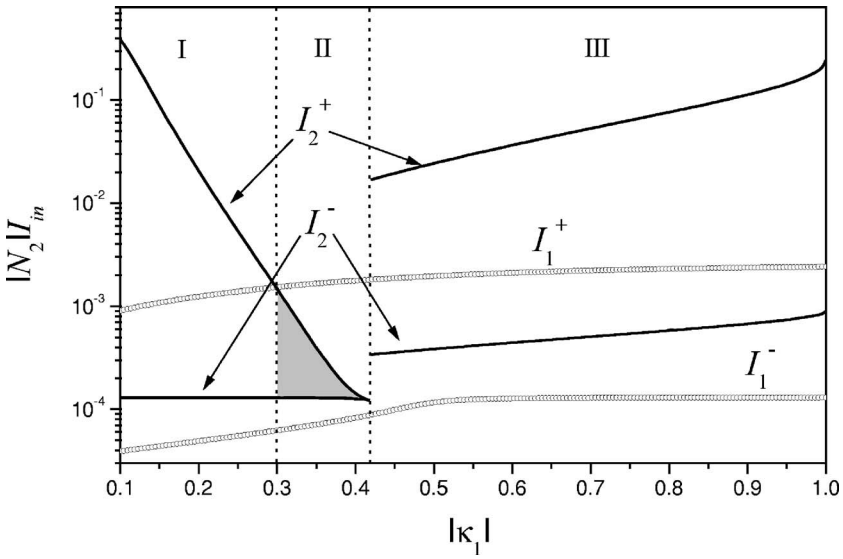

FIG. 8. Switch intensities as a function of the coupling coefficient $|\kappa_1|$ for $\delta > \delta_T$. Solid lines correspond to $I_2^\pm$ and open circles to $I_1^\pm$. The gray area represents the range of κ_1 where $I_2^+ \leqslant I_1^+$.

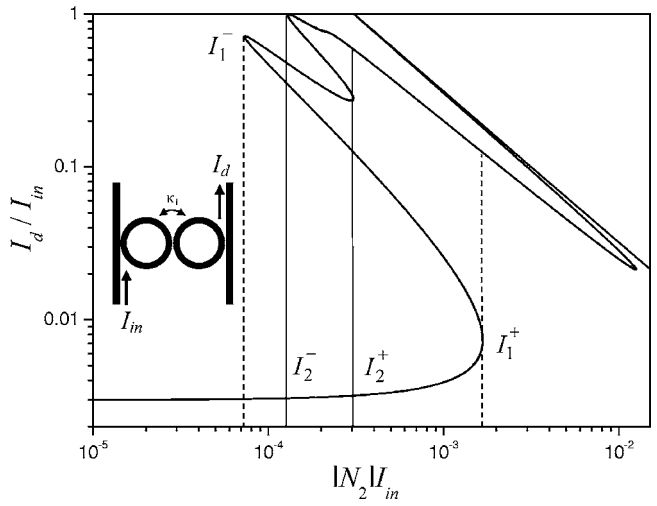

FIG. 9. Transmission as a function of normalized input intensity in the case of two resonators (mean radii $R/2=15\ \mu$m with $\kappa_0=\kappa_2=0.3j$ and $\kappa_1=0.36j$) and a forward-propagating field.

$|\kappa_1|=1$ are similar to those obtained with a single microring (Fig. 6). Figure 9 shows the output port (associated with b_3) transmission as a function of input intensity, with in this case $\kappa_1=0.36j$. This leads to a normalized tristability threshold intensity lower than 0.002 ($|N_2|I_{cav}\sim 0.022$).

For the same configuration ($\kappa_0=\kappa_2=0.3j$), to consider a detuning such as $\delta_B<\delta<\delta_T$ leads to tristability with lower switch intensities for lower $|\kappa_1|$ values (Fig. 10). This occurrence is detrimental to the tristability domain extension. For large $|\kappa_1|$ values the tristability disappears (no overlapping in regime IV). As a general comment we can note that contrary to tristability in single microring (Sec. III A), if we increase the Q factor and choose a related detuning, we can always decrease the bistability and consequently the tristability threshold.

IV. OPTICAL CONTROL OF TRISTABILITY

In Sec. III B we consider a linear coupling between two nonlinear microrings covered by a forward-propagating field. The symmetrical dual-coupling configuration allows us to take the nonlinear coupling between a microring covered by a forward-propagating field and the same microring covered by a backward-propagating field into consideration. The case of both a forward-propagating input a_0' and a backward-propagating control beam c_{N+1} is obtained by a shooting routine. We fix the value of c_{N+1} and $a_{N+1}=0$, we vary b_{N+1}, and we numerically optimize the value of d_{N+1} in order to obtain $c_0'=0$. Consequently it is possible to obtain all the field amplitudes as a function of the fixed parameter c_{N+1} and the varying parameter b_{N+1}. Here we can benefit from the four-value vector associated with the sole nonlinear coupling between forward- and backward-propagating fields. This allows us to identify input and output amplitudes whereas the 2×2 transfer matrix approach as in Fabry-Perot or multilayered media, for fixed forward and backward inputs, and multiple reflections (linear coupling) leads to output indetermination. We consider a single resonator in a similar configuration as in Sec. III A ($\kappa_0=\kappa_1=0.3j$, $L_1=\pi R$) with an input field a_0' and a control beam c_2. We chose $\delta=\omega-\omega_0=0.58\delta_T$ ($\delta>\delta_B$) in order to not observe tristability due to higher-order resonances. The transmission curves in Fig. 11 are obtained with $I_{in}=\frac{1}{2}\epsilon_0 cn_0|a_0'|^2$, $I_d=\frac{1}{2}\epsilon_0 cn_2|b_2|^2$ and different values of $I_c=\frac{1}{2}\epsilon_0 cn_2|c_2|^2$.

Starting from $I_c=0$ [curve (a)] corresponding to a single bistability cycle we can observe how an intermediate stable branch (verifying $dI_d/dI_{in}>0$; see Ref. [7]) with a lower transmission than the initial one appears [curves (b) and (c)]. In the former case (Sec. III B, Fig. 9) the tristability is always obtained with $I_2^->I_1^-$. Here, we can obtain switch intensities such as $I_2^-<I_1^-<I_2^+<I_1^+$ [curve (c)]; in this case, the intermediate stable branch is never reached. The domain of interest corresponds like in Fig. 9 to $I_1^-<I_2^-<I_2^+<I_1^+$ where by decreasing the input power we can reach the intermediate stable branch [curves (d) and (e)]. Alternatively, by turning off the control beam this hysteretic cycle disappears and we recover the standard bistable hysteretic cycle [curve (a)]. In this case the transmission value reached on the intermediate stable branch can be switched to the lowest value. This phenomenon can be used as an optically reconfigurable memory in photonic circuits.

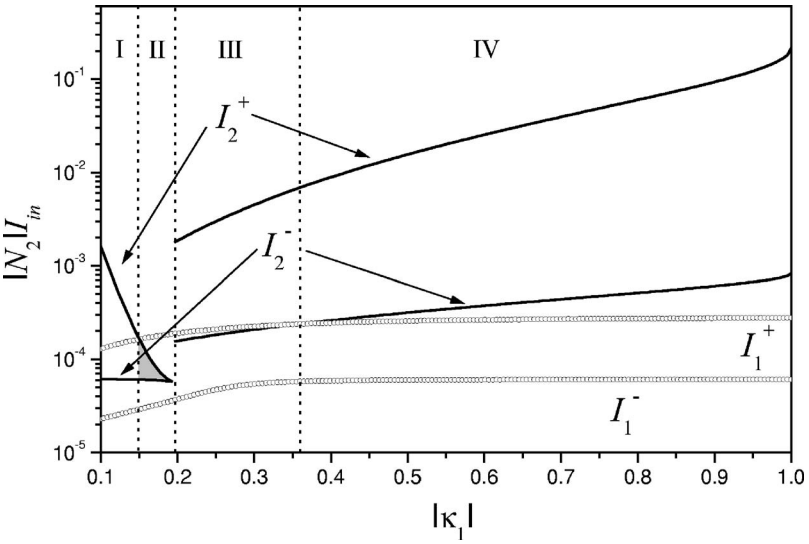

FIG. 10. Switch intensities as a function of the coupling coefficient $|\kappa_1|$ for $\delta_B<\delta<\delta_T$ ($\delta\approx 3\delta_B\approx 0.7\delta_T$). Solid lines correspond to $I_2^\pm$ and open circles to $I_1^\pm$. The gray area represents the range of κ_1 where $I_2^+\leqslant I_1^+$.

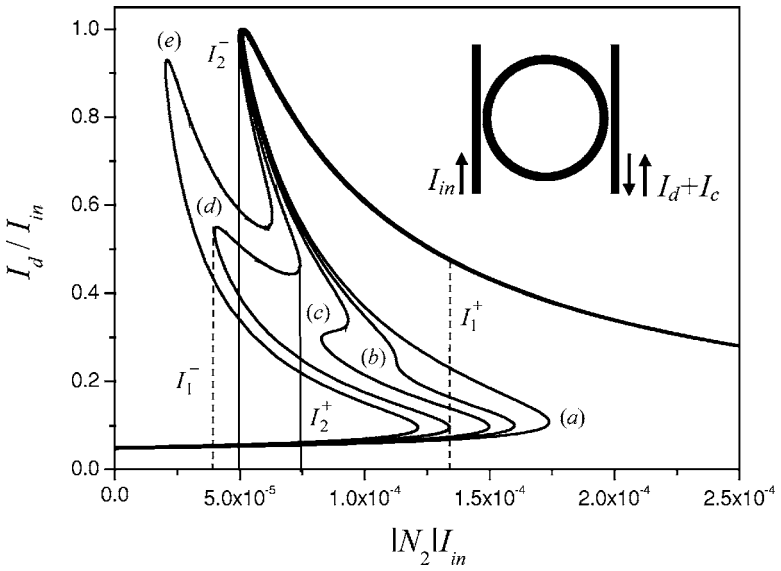

FIG. 11. Normalized output intensity as a function of normalized input intensity for a detuning $\delta=\omega-\omega_0=0.58\delta_T$ in the case of a single microring (mean radius $R=30$ μm with $\kappa_0=\kappa_1=0.3j$). I_c is the control intensity. The different curves are obtained for (a) $|N_2|I_c=0$, (b) $|N_2|I_c=2.5\times10^{-6}$, (c) $|N_2|I_c=5\times10^{-6}$, (d) $|N_2|I_c=10^{-5}$, and (e) $|N_2|I_c=1.5\times10^{-5}$. Switch intensities are represented for case (d).

V. CONCLUSION

In conclusion we have developed a simple four-coupled-mode nonlinear method based on the SVEA. Our approach allows multistability in the presence of independent forward- and backward-propagating fields to be described. We have found a dispersive tristability condition in a single microring resonator. After a study of general families of solutions for a fixed detuning, we have shown how coupling between resonators can be used to reduce the optical power required for dispersive tristability. Finally we propose a method to optically control the multistable behavior of a single resonator. On the contrary to a single microresonator covered by a forward-propagating field, linear or nonlinear coupling between two fields could allow us to consider a higher Q factor in order to decrease the tristability threshold intensity. Using high Q factors would be necessarily associated with the study of dynamic and transient regimes. This would be subject to further work. Our approach can be used to design a realistic device by introducing effective propagation constants β_i^{eff} for WGM's, effective nonlinear indices taking into account transverse profiles of the envelopes $N_{2,i}^{eff}$, and coupling coefficients evaluated by numerical methods [12,16].

ACKNOWLEDGMENTS

We wish to thank S. Bodros for her help in preparing the manuscript and Professor G. M. Stéphan for useful discussions.

[1] D. Sarid, Opt. Lett. **6**, 552 (1981); V. B. Braginsky, M. L. Gorodetsky, and V. S. Ilchenko, Phys. Lett. A **137**, 393 (1989); F. Treussart, V. S. Ilchenko, J.-F. Roch, J. Hare, V. Lefèvre-Seguin, J.-M. Raimond, and S. Haroche, Eur. Phys. J. D **1**, 235 (1998); T. J. Kippenberg, S. M. Spillane, and K. J. Vahala, Phys. Rev. Lett. **93**, 083904 (2004); A. A. Savchenkov, A. B. Matsko, D. Strekalov, M. Mohageg, V. S. Ilchenko, and L. Maleki, *ibid.* **93**, 243905 (2004); H. Rokhsari and K. J. Vahala, Opt. Lett. **30**, 427 (2005).

[2] T. A. Ibrahim, V. Van, and P. T. Ho, Opt. Lett. **27**, 803 (2002).

[3] S. S. Tarng, K. Tai, J. L. Jewell, H. M. Gibbs, A. C. Gossard, S. L. McCall, A. Passner, T. N. C. Venkatesan, and W. Wiegmann, Appl. Phys. Lett. **40**, 205 (1982); O. Sahlén, E. Masseboeuf, M. Rask, N. Nordell, and G. Landgren, *ibid.* **53**, 1785 (1988); B. G. Sfez, J. L. Oudar, J. C. Michel, R. Kuszelewicz, and R. Azoulay, *ibid.* **57**, 1849 (1990).

[4] F. S. Felber and J. H. Marburger, Appl. Phys. Lett. **28**, 731 (1976); J. H. Marburger and F. S. Felber, Phys. Rev. A **17**, 335 (1978).

[5] G. I. Stegeman and C. T. Seaton, J. Appl. Phys. **58**, 57 (1985); H. M. Gibbs, *Optical Bistability: Controlling light with light* (Academic, Orlando, FL, 1985).

[6] A. E. Kaplan and P. Meystre, Opt. Lett. **6**, 590 (1981); E. M. Wright, P. Meystre, W. J. Firth, and A. E. Kaplan, Phys. Rev. A **32**, 2857 (1985); M. Vallet, Ph. Verkerk, and G. Grynberg, Opt. Commun. **75**, 47 (1990).

[7] A. E. Kaplan, Appl. Phys. Lett. **42**, 479 (1983).

[8] G. S. Agarwal and S. Dutta Gupta, Phys. Rev. A **30**, 2764 (1984); G. P. Golubev, D. G. Luchinsky, A. L. Velikovich, and M. A. Liberman, Opt. Commun. **64**, 181 (1987); M. B. Pande, R. Singh, and S. Dutta Gupta, J. Mod. Opt. **40**, 901 (1993); S. Blair, J. E. Heebner, and R. W. Boyd, Opt. Lett. **27**, 357 (2002); J. E. Heebner, R. W. Boyd, and Q.-H. Park, J. Opt. Soc. Am. B **19**, 722 (2002); Y. Chen and S. Blair, Opt. Express **12**, 3353 (2004); S. Pereira, P. Chak, J. E. Sipe, L. Tkeshelashvili, and K. Busch, Photonics Nanostruct. Fundam. Appl. **2**, 181 (2004).

[9] J. Danckaert, K. Fobelets, I. Veretennicoff, G. Vitrant, and R. Reinisch, Phys. Rev. B **44**, 8214 (1991).

[10] J. K. S. Poon, J. Sheuer, S. Mookherjea, G. T. Paloczi, Y. Huang, and A. Yariv, Opt. Express **12**, 90 (2004).

[11] T. Bischofberger and Y. R. Shen, Phys. Rev. A **19**, 1477

(1979); F. J. Fraile-Peláez, M. Prol, D. J. Santos, and J. M. Soto-Crespo, Appl. Phys. Lett. **63**, 1477 (1993); K. Ogusu, H. Shigekuni, and Y. Yokota, Opt. Lett. **20**, 2288 (1995).
[12] Y. Dumeige, C. Arnaud, and P. Féron, Opt. Commun. **250**, 376 (2005).
[13] A. Yariv, Electron. Lett. **36**, 321 (2000).
[14] C. Arnaud, P. Féron, M. Boustimi, P. Grosso, D. Bosc, and P. Guignard, Electron. Lett. **39**, 1249 (2003).
[15] D. D. Smith, H. Chang, and K. A. Fuller, J. Opt. Soc. Am. B **20**, 1967 (2003).
[16] R. Stoffer, K. R. Hiremath, and M. Hammer, in *Microresonators as Building Blocks for VLSI Photonics*, edited by F. Michelotti, A. Driessen, and M. Bertolotti, AIP Conf. Proc. No. 709 (AIP, Melville, NY, 2004), p. 366.